Carbohydrate Polymers 89 (2012) 992–996

Contents lists available at SciVerse ScienceDirect

Carbohydrate Polymers

journal homepage: www.elsevier.com/locate/carbpol

Short communication

Preparation and characterization of cellulose/hydrous niobium oxide hybrid

Leandro José Maschio[a,*], Paulo Henrique Fernandes Pereira[b], Maria Lucia Caetano Pinto da Silva[a]

[a] Chemistry Department – DEQUI/EEL/USP. Rod. Itajubá-Lorena, Km 74,5 – Lorena – Cep: 12600 000 – SP – Brazil
[b] Fatigue and Aeronautical Materials Research Group – DMT/FEG/UNESP. Av. Ariberto Pereira da Cunha, 333 – Guaratinguetá – Cep: 12516 410 – SP – Brazil

ARTICLE INFO

Article history:
Received 28 September 2011
Received in revised form 13 February 2012
Accepted 4 April 2012
Available online 22 April 2012

Keywords:
Cellulose
Hydrous niobium oxide
Sugarcane bagasse

ABSTRACT

A composite of cellulose extracted from bagasse with $Nb_2O_5 \cdot nH_2O$ in three different proportions (16.67, 37.5 and 50.0 wt%) was prepared using the co-precipitation method. The materials were characterized by X-ray diffractometry (XRD), Fourier transform infra-red spectroscopy (FTIR), thermogravimetric analysis (TG/DTG), differential scanning calorimetry (DSC) and scanning electron microscopy (SEM). TG data obtained show that the presence of inorganic material influenced slightly the stability of the hybrid material. The precipitation of 16.67 wt.% of oxide was sufficient to inhibit the combustion peaks present in the DSC curve of cellulose. This work will help find new applications for these materials.

1. Introduction

Sugarcane bagasse is a fibrous material mainly composed of cellulose, hemicelluloses, and lignin (Miretzky & Cirelli, 2010; Viera et al., 2007; Wang, Li, Xiao, & Wu, 2009). According to Mulinari, Voorwald, Cioffi, Silva, and Luz (2009), this agro-industrial residue contains cellulose (46.0%), hemicellulose (24.5%), lignin (19.95%), fat and waxes (3.5%), ash (2.4%), silica (2.0%) and other elements (1.7%). World production of sugarcane bagasse is between 320 million to 380 million tons per year according to Abbasi and Abbasi (2010). The use of waste as raw material for various chemical processes already occurs, but a large amount is still not reused (Pantoja, Sader, Damianovic, Foresti, & Silva, 2010). Due to the large amount of bagasse produced, there has been a growing trend towards the development and optimization of processes using this industrial waste as raw material.

More recently, particular attention has been directed to the development of nanocomposites based on cellulose and inorganic nanoparticles, such as SiO_2, TiO_2, $CaCO_3$, $NbOPO_4 \cdot nH_2O$, among others (Maliyekkal, Lisha, & Pradeep, 2010; Pereira, Voorwald, Cioffi, & Silva, 2010a; Pinto, Marques, Barros-Timmons, Trindade, & Pascoal Neto, 2008; Vilela et al., 2010; Xie, Yu, & Shi, 2009), because these materials normally have improved mechanical, optical and thermal properties due to the combination of inorganic and organic components.

Organic–inorganic hybrid materials are of more than academic interest, since their inherent properties frequently lead to the development of innovative industrial applications. Such fields as optics, electronics, ionics, mechanics, energy, environment, biology, medicine, smart coatings, fuel and solar cells, catalysts, sensors, fire retardant, production of composites or membranes are some examples of promising applications areas where these types of materials have been successfully applied (Pereira, Voorwald, Cioffi, & Silva, 2011).

The world's 5th largest country in terms of its area, and rich in natural resources, Brazil's economy is based on the exploration of both renewable and non-renewable resources. It is the world's leading producer of niobium (Tanimoto, Durany, Villalba, & Pires, 2010; Vilela et al., 2010). Its niobium reserves totaled 842.46 million tons and are concentrated in the states of Minas Gerais (75.08%), Amazonas (21.34%) and Goiás (3.58%) (DNPM, 2009). Thus, hydrous niobium oxide has shown to be an attractive alternative to the inorganic portion in the preparation of organic–inorganic hybrids. In this work, the objective of this paper is to prepare and characterize cellulose/$Nb_2O_5 \cdot nH_2O$ hybrids by X-ray diffratometry (XRD), Fourier transform infra-red spectroscopy (FTIR), thermogravimetric analysis (TG/DTG), differential scanning calorimetry (DSC) and scanning electron microscopy (SEM). The proposed application of the materials prepared in this study is their use as additives in polymer matrices and inorganic membranes.

2. Experimental

2.1. Preparation of the bleached cellulose

The bagasse was pretreated with a 10% sulfuric acid solution in 350 L stainless reactor for 10 min, with solid/liquid of 1:20 (w/v). Therefore, we obtained cellulose and lignin free of hemicellulose.

* Corresponding author.
E-mail address: ljmaschio@gmail.com (L.J. Maschio).

0144-8617 Published by Elsevier Ltd. Open access under the Elsevier OA license.
http://dx.doi.org/10.1016/j.carbpol.2012.04.043

The cellulignin was submitted in alkaline in a 350 L stainless reactor with 150 L of destilled water, 10 kg pretreatead sugarcane bagasse and 30 L of aqueous solution containning 3 kg NaOH. The reaction was performed at 100 °C for 1 h under stirring at 100 rpm. The final concentration of the mixture was 1.5 wt% NaOH and solid/liquid ratio of 1:20 (w/v), obtained a crude pulp (Pereira et al., 2010a; Rocha, 2000).

2.2. Preparation of the cellulose/hydrous niobium oxide hybrids

Cellulose/$Nb_2O_5{\cdot}nH_2O$ hybrids were prepared in three different proportions 16.67, 37.5 and 50.0 wt.%. These materials were prepared by a co-precipitation method. The dissolution of metallic niobium was held in a polyethylene becker with nitric and hydrofluoric acid, both concentrated, with a molar relation of $1HF:3HNO_3$. Then, to this solution was added cellulose with 140 mL of deionized water. Then excess of ammonium hydroxide solution (1:3 molar) was added dropwise to the solution with constant stirring at room temperature until a crystalline precipitation was formed into cellulose. After the precipitation, the materials were washed several times until pH ~7 with deionized water and dried in oven at 50 °C until a constant weight was achieved.

2.3. Characterization of the materials

The hydrous niobium oxide, the cellulose and the hybrids Cellulose/$Nb_2O_5{\cdot}nH_2O$ were characterized by X-ray diffratometry (XRD), Fourier transform infra-red spectroscopy (FTIR), thermogravimetric analysis (TG/DTG), differential scanning calorimetry (DSC) and scanning electron microscopy (SEM).

X-ray diffractograms were obtained with a Rich Seifert diffractometer model XRD6000 with radiation CuKα, tension of 30 kV, current of 40 mA, and 0.05 (2θ/5 s) scanning from values of 2θ it enters 10–70° (2θ).

FTIR spectra of hydrous niobium oxide, cellulose and cellulose/$Nb_2O_5{\cdot}nH_2O$ hybrids were obtained in a FTIR spectrophotometer Perkin Elmer. The powered samples were mixed with KBr to produce tablets. The scan was performed in the spectral range of 4000–400 cm^{-1}.

Thermogravimetric analyses (TG/DTG) were carried with a Shimadzu TGA-50 thermal analyzer from room temperature to 900 °C at a heating of 20 °C min^{-1} in N_2 atmosphere.

DSC analysis was performed using a calorimetric instrument Seiko Instruments model Exstar 6000, by the heat of the sample 5 mg in temperatures between 25 and 550 °C, rates under oxygen atmosphere at a range 10 °C min^{-1}.

Surface materials were examined by Scanning Electron Microcopy (SEM) a JEOL JSM5310 model. Samples to be observed under the SEM were mounted on conductive adhesive tape, sputter coated with gold and observed in the SEM using a voltage of 15 kV.

3. Results and discussion

X-Ray diffraction (XRD) patterns were used to investigate the crystallinity of the materials. In Fig. 1 presented the X-ray diffractograms of cellulose, $Nb_2O_5{\cdot}nH_2O$ and hybrids materials. Differences between cellulose and hybrid material can be observed in the X-ray diffractograms shown in Fig. 1.

It is possible to observe a change in the intensity of the peaks found between diffraction at the following 2θ angles: 16.3°, 22.8° and 28°. The strongest cellulose peak, at $2\theta = 22.8°$, originates from the cellulose crystalline plane 0 0 2 (Zhao et al., 2007) and the peak at $2\theta = 16.3°$ corresponds to the cellulose (1 0 1) crystallographic planes. The diffractograms, probably representing typical cellulose I diffractograms, show a peak at $22 < 2\theta < 23°$ and a shoulder in the region $2\theta = 14–17°$ (Elanthikkal, Gopalakrishnapanicker, Varghese, & Guthrie, 2010), and common crystal formation was observed in native cellulose (Zhang et al., 2010). Fig. 1 shows the changes as the amount of deposited oxides increases.

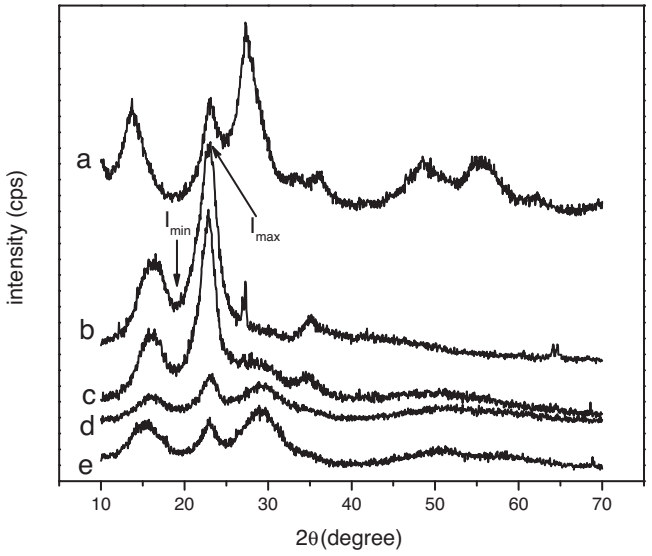

Fig. 1. X-ray diffractogram of $Nb_2O_5{\cdot}nH_2O$ (a), cellulose (b), hybrid 16.67 wt.% (c), hybrid 37.5 wt.% (d), hybrid 50 wt.% (e).

Through DRX curves was calculated the crystallinity index (I_{cr}) of the materials. I_{cr} was calculated as the ratio of the intensity differences in the peak positions at 18° and 22° according to Eq. (1) (Ass, Belgacem, & Frollini, 2006; Guimarães, Frollini, Silva, Wypych, & Satyanarayana, 2009; Pereira et al., 2010a).

$$I_{cr} = 1 - \frac{I_{min}}{I_{max}} \quad (1)$$

where I_{min} is the intensity at minimum of the crystalline peak ($18° < 2\theta < 19°$) and I_{max} is the intensity at its maximum ($22° < 2\theta < 23°$). According to this method, the degree of crystallinity was calculated (Table 1).

With the increased $Nb_2O_5{\cdot}nH_2O$ into cellulose surface loading occurred a decreased in the intensity of peaks corresponding to cellulose, when compared with the peak related to metallic oxide, resulting in a diminution of the relationship between amorphous and crystalline phase of the fiber, which caused a decrease in the crystallinity index materials.

The Fig. 2 shows the consequences arising from the heating and subsequent thermal degradation of the materials studied.

TG curve in Fig. 2a of the hydrous niobium oxide shows a weight loss occurring in two distinct stages within the temperature range of 25–800 °C. In the first one, between the temperature of 40 °C and 170 °C, was caused by desorption of physically adsorbed water (Rodrigues & Silva, 2009). The weight loss on the second step was caused by the hydroxyl groups' condensation. TG curve in Fig. 2b for the cellulose shows three weight loss steps. The first is attributed to desorption of water from the polysaccharide structure (Bertoti, Luporini, & Esperidião, 2009). The second step (182–404 °C) can be assigned to the decomposition of the cellulose and lignin portion. The third step (404–736 °C) corresponds

Table 1
Crystallinity index for the cellulose and Cell/$Nb_2O_5{\cdot}nH_2O$ hybrids.

Material	Degree crystallinity (%)
Cellulose	71.30
Cell/$Nb_2O_5{\cdot}nH_2O$ 16.67 wt.%	70.89
Cell/$Nb_2O_5{\cdot}nH_2O$ 37.50 wt.%	58.92
Cell/$Nb_2O_5{\cdot}nH_2O$ 50.00 wt.%	53.11

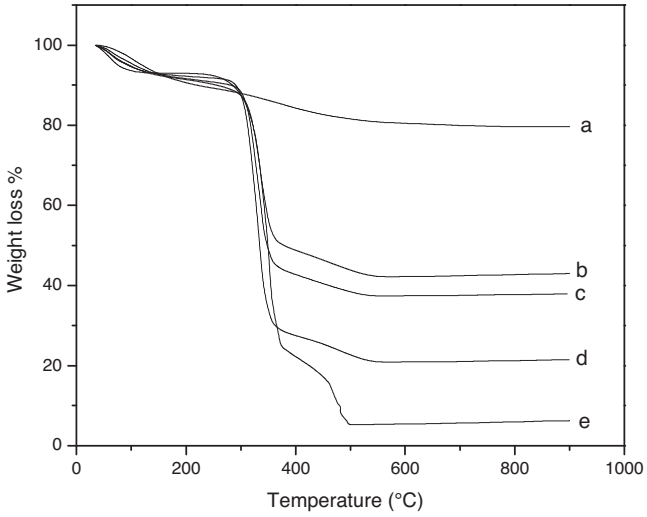

Fig. 2. TG curves of $Nb_2O_5{\cdot}nH_2O$ (a), cellulose (b), hybrid 16.67 wt.% (c), hybrid 37.5 wt.% (d) and hybrid 50 wt.% (e).

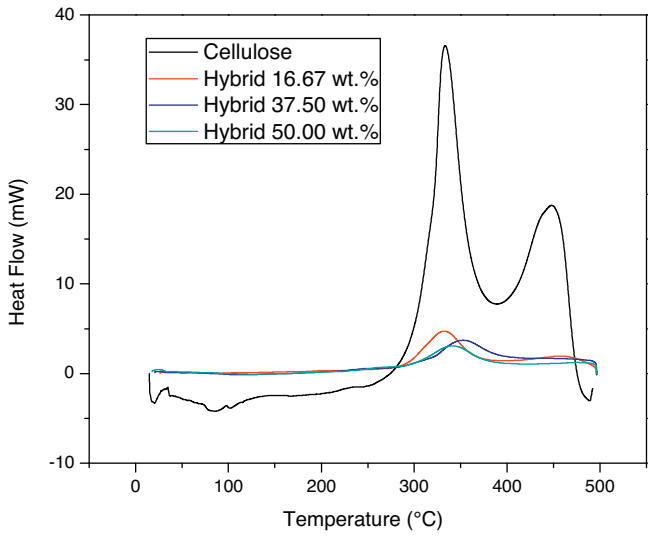

Fig. 3. DSC curves of $Nb_2O_5{\cdot}nH_2O$, cellulose, hybrid 16.67 wt.%, hybrid 37.5 wt.% and hybrid 50 wt.%.

to the residual lignin decomposition reactions degradation (Yang, Yan, Chen, Lee, & Zheng, 2007).

From Table 2, it may be observed a progressive increase in percentage of the residue with an increase of $Nb_2O_5{\cdot}nH_2O$ in respect to the pureness cellulose that indicated the presence of inorganic material. This higher amount of remaining residue confirmed the presence of hydrous niobium oxide on the cellulose surface. In Fig. 2, it is shown that the presence of inorganic material slightly influenced the stability of hybrid material. TG curves shows that the hybrid 50.00 wt.% is the best of them because present the minor dm in the second step. This case is attributed the more interaction cellulose–hydrous niobium oxide.

DSC analysis in oxygen showed that active combustion took place at 275 °C and ended at 475 °C with two major peaks at 331 and 446 °C. During the thermal degradation of cellulose, depolymerization occurs and formation of 1.6 anhydro-glucose takes place and its decomposition involves the formation of volatiles. The formation of volatile products during the degradation cellulose is indicated by the exothermic peak at 35 °C and 275 °C in DSC curve of cellulose.

The first exothermic event refers to the steps that can be related to flaming combustion of the volatiles. In this peak the value of enthalpy is higher for the cellulose. Enthalpy values for the hybrids show that the deposition of $Nb_2O_5{\cdot}nH_2O$ significantly reduced the enthalpy in relation to cellulose.

The second exothermic peak was attributed to char oxidation. In hybrids cell/$Nb_2O_5{\cdot}nH_2O$ (Lee, Chen, & Rowell, 2004), this second event is not present, which may be explained by the presence of hydrous niobium oxide on the fiber surface, which inhibited the same and acted as a flame retardant.

In Fig. 3, it may be noted that the increase $Nb_2O_5{\cdot}nH_2O$ loading does not cause significant changes in the DSC curves. Therefore, the precipitation of 16.67 wt.% of oxide was sufficient to inhibit the combustion peaks present in the DSC curve of cellulose.

The FTIR spectra for the samples are shown in Fig. 4. Many differences between cellulose and hybrids materials can be observed in the FTIR spectra of the studied materials.

It is possible to observe a major absorption of peaks of 3400, 1385, 1643, and 650 cm^{-1}. The position 3400 cm^{-1} corresponds to O–H stretching vibration. This increase absorption in 3400 cm^{-1} showed an increase hydrophilic character of the fiber with the

Table 2
Results of TG curves with the corresponding temperatures to the maximum rate of mass loss in (dm) in the respective intervals of temperature (ΔT) with losses of mass in TG (Δm) and residue (R).

Material	Δm (%)	ΔT (°C)	dm (°C)	R (%)
	10.87	36–254	107	79.66
$Nb_2O_5{\cdot}nH_2O$	9.47	254–850	367	
Crude pulp	8.42	35–182	64	3.62
	72.18	182–404	358	
	15.78	404–736	438	
Hybrid 16.67 wt.%	4.45	39–144	65	16.95
	65.21	144–407	341	
	13.39	407–681	485	
Hybrid 37.50 wt.%	7.58	33–176	62	37.42
	5.14	176–283	271	
	42.15	283–418	340	
	7.71	418–665	494	
Hybrid 50.00 wt.%	6.23	35–170	65	45.86
	8.65	170–294	267	
	32.16	294–427	342	
	7.10	427–665	497	

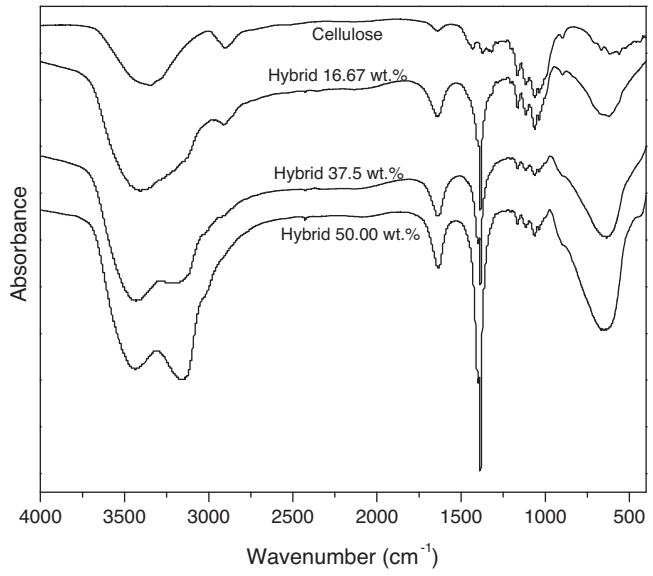

Fig. 4. FTIR spectra of $Nb_2O_5{\cdot}nH_2O$ (a), cellulose (b), hybrid 16.67% (c), hybrid 37.5 wt.% (d), hybrid 50 wt.% (e).

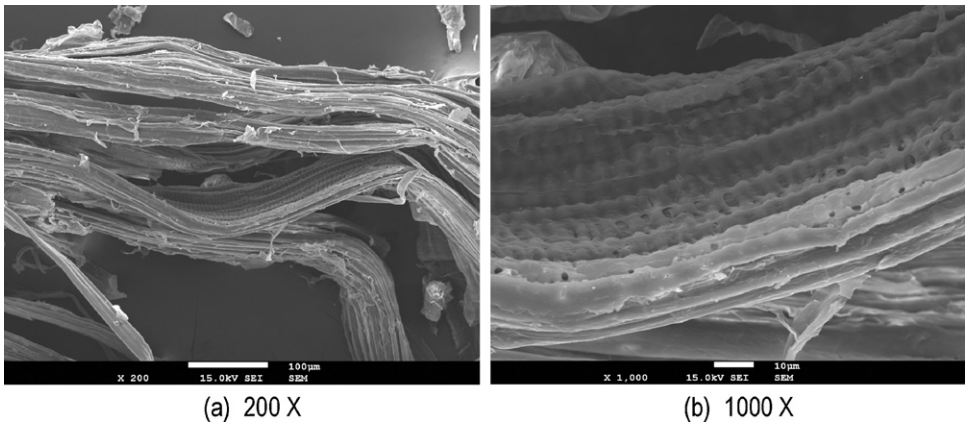

Fig. 5. SEM cellulose fibers with 200× (a), 1000× (b).

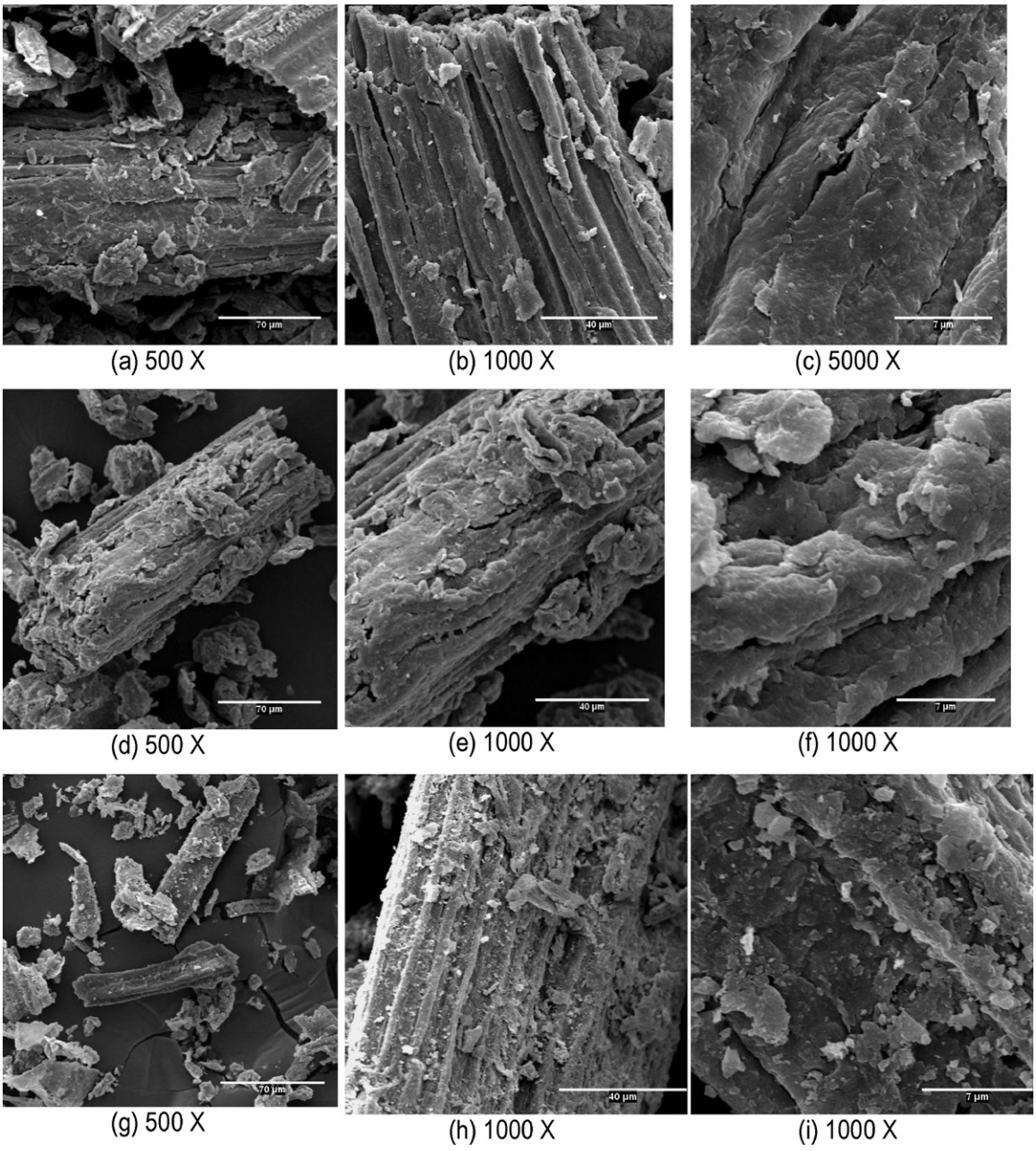

Fig. 6. SEM, hybrid 16.67 wt.% (a–c), hybrid 37.5 wt.% (d–f) and hybrid 50 wt.% (g–i).

increasing incorporation of $Nb_2O_5{\cdot}nH_2O$ onto the fibers. The peak at 2900 cm^{-1} indicates the absorption region of the symmetrical stretching C–H of polysaccharides. Increasing oxide loading generates a reduction in the absorption of this peak. The peak at 1640 cm^{-1} is attributable to a vibration of OH groups from water (Mulinari et al., 2009; Pereira et al., 2010b). The intensity of this peak is higher for the hybrid 50.00%, which can be explained by the fact that the amount of hydration water present is higher. The peak at 1385 cm^{-1} indicated the presence of surface hydroxyl on the metal oxide surface. The characteristic absorption in the range of 900–500 cm^{-1} is attributable to vibration Nb–O vibration (Rodrigues & Silva, 2010).

According to Reddy and Yang (2005), in general all natural cellulose fibers are multi-cellular, where a bundle of individual cells bound by natural polymers such as lignin and pectin. The scanning electron micrographs presented in Fig. 5 shows cellulose fibers that are packed together. The Fig. 5b shows photomicrographs of the cellulose fibers and the presence of "pits" longitudinally arranged along the entire cell wall, the inside and outside the parenchyma cells of fibers that are responsible for transportation water and nutrients throughout various cells to the roots and leaves. For oxide deposition on the fibers, it is interesting to observe a large area and roughness on the surface.

The micrographs in Fig. 6 shows of different magnification of the hybrids materials prepared (hybrid 16.67 wt.%, 37.50 wt.% and 50.00 wt.%). Observed hydrous niobium oxide was dispersed on the cellulose surface. Fig. 6h clearly shows that deposition of inorganic material. The deposition was on a no-homogenous surface of the cellulose fiber. From EDS analyses the presence of the elements niobium and oxygen was confirmed. EDS analysis indicate which all the sulfur acid utilized in the treatment of the fiber was removed during the washing with deionized water.

4. Conclusions

With the increased $Nb_2O_5{\cdot}nH_2O$ in cellulose surface loading, a decrease in the crystallinity index materials occurred. The presence of the metallic oxide influences significantly the thermal stability of hybrid materials. According to the results of TG, the hybrid one which contains 50.00% $Nb_2O_5{\cdot}nH_2O$ presents advantages on others studied proportions. The lower quantity of oxides was enough in order to inhibit the combustion peaks of cellulose present in the DSC graphics, but the results show that the deposition of 50.00% $Nb_2O_5{\cdot}nH_2O$ provides to total inhibition of these peaks.

Through the FTIR spectra, a specific absorption region could be observed between 900–500 cm^{-1} atributed to the Nb–O vibration. SEM images show a non-homogenous deposition of $Nb_2O_5{\cdot}nH_2O$ on the surface of the cellulose matrix. SEM and EDS confirm the presence of $Nb_2O_5{\cdot}nH_2O$ on the surfaces of the fibers.

References

Abbasi, T., & Abbasi, S. A. (2010). Biomass energy and the environmental impacts associated with its production and utilization. *Renewable and Sustainable Energy Reviews*, *14*, 919–937.

Ass, B. A. P., Belgacem, M. N., & Frollini, E. (2006). Mercerized linters cellulose: characterization and acetylation in *N*-*N*-dimethylacetamide/lithium chloride. *Carbohydrate Polymers*, *63*, 19–29.

Bertoti, A. R., Luporini, S., & Esperidião, M. C. A. (2009). Effects of acetylation in vapor phase and mercerization on the properties of sugarcane fibers. *Carbohydrate Polymers*, *77*, 20–24.

DNPM Economia Mineral do Brasil 2009, DNPM, Brasília (2009). Internet file, URL http://www.dnpm.gov.br.

Elanthikkal, S., Gopalakrishnapanicker, U., Varghese, S., & Guthrie, J. T. (2010). Cellulose microfibres produced from banana plant wastes: isolation and characterization. *Carbohydrate Polymers*, *80*, 852–859.

Guimarães, J. L., Frollini, E., Silva, C. G., Wypych, F., & Satyanarayana, K. G. (2009). Characterization of banana, sugarcane bagasse and sponge gourd fibers of Brazil. *Industrial Crops and Products*, *30*, 407–415.

Lee, H. L., Chen, G. C., & Rowell, R. M. (2004). Thermal properties of wood reacted with a phosphorous pentoxide–amine system. *Journal of Applied Polymer Science*, *91*, 2465–2481.

Maliyekkal, S. M., Lisha, K. P., & Pradeep, T. (2010). A novel cellulose–manganese oxide hybrid material by in situ soft chemical synthesis and its application for the removal of Pb(II) from water. *Journal of Hazardous Materials*, *181*, 986–995.

Miretzky, P., & Cirelli, A. F. (2010). Cr(VI) and Cr(III) removal from aqueous solution by raw and modified lignocellulosic materials: a review. *Journal of Hazardous Materials*, *180*, 1–19.

Mulinari, R. M., Voorwald, H. C. J., Cioffi, M. O. H., Silva, M. C. P., & Luz, S. M. (2009). Preparation and properties of HDPE/sugarcane bagasse cellulose composites obtained for thermokinetic mixer. *Carbohydrate Polymers*, *75*, 317–321.

Pantoja, J. L. R., Sader, L. T., Damianovic, M. H. R. Z., Foresti, E., & Silva, E. L. (2010). Performance evaluation of packing materials in the removal of hydrogen sulphide in gas-phase biofilters: polyurethane foam, sugarcane bagasse, and coconut fibre. *Chemical Engineering Journal*, *158*, 441–450.

Pereira, P. H. F., Voorwald, H. C. J., Cioffi, M. O. H., & Silva, M. L. C. P. (2010). Preparation and characterization of cellulose/hydrous niobium phosphate hybrid. *BioResources*, *5*(2), 1010–1021.

Pereira, P. H. F., Voorwald, H. C. J., Cioffi, M. O. H., Mulinari, D. R., Luz, S. M., & Silva, M. L. C. P. (2010). Sugarcane bagasse pulping and bleaching: thermal and chemical characterization. *BioResources*, *6*(3), 2471–2482.

Pereira, P. H. F., Voorwald, H. C. J., Cioffi, M. O. H., & Silva, M. L. C. P. (2011). Novel cellulose/$NbOPO_4{\cdot}nH_2O$ hybrid material from sugarcane bagasse. *BioResources*, *6*(1), 867–878.

Pinto, R. J. B., Marques, P. A. A. P., Barros-Timmons, A. M., Trindade, T., & Pascoal Neto, C. (2008). Novel SiO_2/cellulose nanocomposites obtained by in situ synthesis and via polyelectrolytes assembly. *Composites Science and Technology*, *68*, 1088–1093.

Reddy, N., & Yang, Y. (2005). Biofibers from agricultural byproducts for industrial applications. *TRENDS in Biotechnology*, *23*(1), 22–27.

Rocha, G. J. M. (2000). *Deslignificação de bagaço de cana de açúcar assistida por oxigênio*. Doctoral thesis. São Carlos, USP, p. 136.

Rodrigues, L. A., & Silva, M. L. C. P. (2009). An investigation of phosphate adsorption from aqueous solution onto hydrous niobium oxide prepared by co-precipitation method. *Colloids and Surfaces A: Physicochemical Engineering Aspects*, *334*, 191–196.

Rodrigues, L. A., & Silva, M. L. C. P. (2010). Synthesis of $Nb_2O_5{\cdot}nH_2O$ nanoparticles by water-in-oil microemulsion. *Journal of Non-Crystalline Solids*, *356*, 125–128.

Tanimoto, A. H., Durany, X. G., Villalba, G., & Pires, A. C. (2010). Material flow accounting of the copper cycle in Brazil. *Resources, Conservation and Recycling*, *55*, 20–28.

Viera, R. G. P., Rodrigues Filho, G., Assunção, R. M. N., Meireles, C. S., Vieira, J. G., & Oliveira, G. S. (2007). Synthesis and characterization of methylcellulose from sugar cane bagasse cellulose. *Carbohydrate Polymers*, *67*, 182–189.

Vilela, C., Freire, C. S. R., Marques, P. A. A. P., Trindade, T., Pascoal Neto, C., & Fardim, P. (2010). Synthesis and characterization of new $CaCO_3$/Cellulose nanocomposites prepared by controlled hydrolysis of dimethylcarbonate. *Carbohydrate Polymers*, *79*, 1150–1156.

Wang, Z. M., Li, L., Xiao, K. J., & Wu, J. W. (2009). Homogeneous sulfation of bagasse cellulose in an ionic liquid and anticoagulation activity. *Bioresource Technology*, *100*, 1687–1690.

Xie, K., Yu, Y., & Shi, Y. (2009). Synthesis and characterization of cellulose/silica hybrid materials with chemical crosslinking. *Carbohydrate Polymers*, *78*, 799–805.

Yang, H., Yan, R., Chen, H., Lee, D. H., & Zheng, C. (2007). Characteristics of hemicellulose, cellulose and lignin pyrolysis. *Fuel*, *86*, 1781–1788.

Zhao, H., Kwak, J. H., Wang, Y., Franz, J. A., White, J. M., & Holladay, J. E. (2007). Interactions between cellulose and N-methylmorpholine-N-oxide. *Carbohydrate Polymers*, *67*, 97–103.

Zhang, J., Luo, J., Tong, D., Zhu, L., Dong, L., & Hu, C. (2010). The dependence of pyrolysis behavior on the crystal state of cellulose. *Carbohydrate Polymers*, *79*, 164–169.